An Alternative Explanation for the Catalytic Proficiency of Orotidine 5′-Phosphate Decarboxylase

Tai-Sung Lee,*,†,‡ Lillian T. Chong,§ John D. Chodera,§ and Peter A. Kollman‡

Contribution from Accelrys, Inc., 9685 Scranton Road, San Diego, California 92121-3752, and Department of Pharmaceutical Chemistry and Graduate Group in Biophysics, University of California, San Francisco, California 94143-0446

Received April 30, 2001

Abstract: Orotidine 5′-phosphate decarboxylase (ODCase) is the most proficient enzyme known, enhancing the rate of decarboxylation of orotidine 5′-phosphate (OMP) by a factor of 10^{17}, which corresponds to a $\Delta\Delta G^{\ddagger}$ of ∼24 kcal/mol. Ground-state destabilization through local electrostatic stress has been recently proposed as the basis of catalytic rate enhancement for a mechanism that is the same as in solution. We have carried out gas-phase *ab initio* quantum mechanical calculations combined with a free energy method, a continuum solvent model, and molecular dynamics simulations to assess an alternative mechanism. Although we are not able to reproduce the experimentally observed $\Delta\Delta G^{\ddagger}$ quantitatively, we present evidence that this $\Delta\Delta G^{\ddagger}$ is very large, in the range found experimentally. We thus conclude that the preferred mechanism may well be different from that in solution, involving an equilibrium pre-protonation of OMP C5 by a catalytic lysine residue that greatly reduces the barrier to subsequent decarboxylation.

1. Introduction

Orotidine 5′-phosphate decarboxylase (ODCase) catalyzes the decarboxylation of orotidine 5′-phosphate (OMP), the final step in the *de novo* biosynthesis of uridine 5′-phosphate (UMP). This dimeric enzyme is unusually proficient, enhancing the rate of decarboxylation by a factor of 10^{17}, which corresponds to a $\Delta\Delta G^{\ddagger}$ of ∼24 kcal/mol[1] in neutral solution at room temperature. No cofactors or metals are involved in the catalysis. To explain the enzyme's proficiency, numerous mechanisms have been proposed based on model systems, kinetic isotope experiments, and, more recently, crystal structures.

The first set of mechanisms were proposed prior to the availability of the enzyme crystal structures. Beak and Siegel[2] suggested a zwitterion mechanism where O2-protonation of OMP yields an ylide intermediate, which acts as an electronic sink. Silverman and Groziak[3] proposed a nucleophilic addition to C5 of the substrate by an active site residue, which is then expelled upon decarboxylation. On the basis of quantum mechanical calculations, Lee and Houk[4] proposed a mechanism involving O4-protonation concerted with decarboxylation via a carbene intermediate. Their results indicated that O4-protonation lowered the activation free energy for decarboxylation from a computed value of 42 kcal/mol in solution to 18 kcal/mol in the enzyme environment, which was modeled as a bulk medium with dielectric constant 4. A fourth proposal involved a modified version of this mechanism by Ehrlich *et al.*,[5] who conducted multiple solvent deuterium and ^{13}C kinetic isotope effect experiments on catalysis by ODCase. Their results indicate that catalysis involves a stepwise mechanism in which a protonation event occurs prior to decarboxylation. This led them to propose O4-protonation followed by decarboxylation.

Kinetic isotope studies have provided evidence against mechanisms involving either nucleophilic addition to C5 of the substrate or O4-protonation. When the substrate was synthesized with deuterium at C5, Acheson *et al.*[6] observed no secondary deuterium isotope effect, thereby providing no support for mechanisms involving nucleophilic addition to C5 of the substrate. Furthermore, the observation by Smiley *et al.*[7] of a large ^{13}C isotope effect in the enzymatic reaction has established that decarboxylation is the rate-determining step, thus suggesting that no covalent step, unless it is fast (e.g., a proton-transfer event), occurs before decarboxylation. The O4-protonation mechanisms are unlikely due to the finding by Shostak and Jones[8] of a large effect on the reaction rate (greater than 10 000-fold reduction in k_{cat}) with an O2 → S2 substitution and only a small effect on the rate (50% reduction in k_{cat}) with an O4 → S4 substitution.

Recent crystal structures of ODCase from four different microbial sources in complexes with various inhibitors[9−13] have provided evidence against all of the mechanisms described

* To whom correspondence should be addressed.
† Accelrys, Inc.
‡ Department of Pharmaceutical Chemistry, UCSF.
§ Graduate Group in Biophysics, UCSF.

(1) Radzicka, A.; Wolfenden, R. *Science* **1995**, *267*, 90−93.
(2) Beak, P.; Siegel, B. *J. Am. Chem. Soc.* **1976**, *98*, 3601−3606.
(3) Silverman, R.; Groziak, M. *J. Am. Chem. Soc.* **1982**, *104*, 6434−6439.
(4) Lee, J.; Houk, K. *Science* **1997**, *276*, 942−945.
(5) Ehrlich, J.; Hwang, C.; Cook, P.; Blanchard, J. *J. Am. Chem. Soc.* **1999**, *121*, 6966−6967.
(6) Acheson, S.; Bell, J.; Jones, M.; Wolfenden, R. *Biochemistry* **1990**, *29*, 3198−3202.
(7) Smiley, J.; Paneth, P.; Oleary, M.; Bell, J.; Jones, M. *Biochemistry* **1991**, *30*, 6216−6223.
(8) Shostak, K.; Jones, M. *Biochemistry* **1992**, *31*, 12155−12161.
(9) Appleby, T.; Kinsland, C.; Begley, T.; Ealick, S. *Proc. Natl. Acad. Sci. U.S.A.* **2000**, *97*, 2005−2010.
(10) Harris, P.; Poulsen, J.; Jensen, K.; Larsen, S. *Biochemistry* **2000**, *39*, 4217−4224.
(11) Feng, W.; Austin, T.; Chew, F.; Gronert, S.; Wu, W. *Biochemistry* **2000**, *39*, 1778−1783.
(12) Miller, B.; Hassell, A.; Wolfenden, R.; Milburn, M.; Short, S. *Proc. Natl. Acad. Sci. U.S.A.* **2000**, *97*, 2011−2016.
(13) Wu, N.; Mo, Y.; Gao, J.; Pai, E. *Proc. Natl. Acad. Sci. U.S.A.* **2000**, *97*, 2017−2022.

10.1021/ja011096f CCC: $20.00
Published on Web 12/19/2001

above. The structures reveal no polar or charged residues near O2 or O4 of the substrate, thereby ruling out O2-protonation and O4-protonation mechanisms. Mechanisms involving nucleophilic addition to C5 are also unlikely due to the absence of a nucleophile near C5 of the substrate. In the vicinity of C5, however, is Lys72 (*Methanobacterium autotrophicum* numbering[13]), which has been revealed by site-directed mutagenesis to be an essential proton-donating catalytic residue that does not appear to be critical for substrate binding.[14] This catalytic residue is part of a unique, conserved Lys42-Asp70-Lys72-Asp75B charged array that lines the pocket for the substrate carboxylate group (Asp75B is from the adjacent monomer).

Various mechanisms have been proposed based on the crystal structures.[15] Wu *et al.*[16] and Appleby *et al.*[9] have interpreted the crystal structures as evidence for ground-state destabilization by the severe repulsion between the carboxylate of the substrate and the anionic form of Asp70. In the transition state, this charge repulsion would be diminished due to a decreased anionic character of the substrate carboxylate group. Wu *et al.*[16] have suggested that ground-state destabilization drives unimolecular cleavage of the bond between C6 and the carboxylate carbon of the substrate, which is followed by protonation of C6 by Lys72. Using hybrid quantum mechanical/molecular mechanics (QM/MM) calculations, they find that the "electrostatic stress" free energy of 18 kcal/mol between the substrate carboxylate and Asp70 is compensated by the strong binding of the phosphoribosyl region, computed to be −26 kcal/mol. Appleby *et al.*[9] have proposed an electrophilic substitution mechanism in which C6-protonation and decarboxylation occur in a concerted manner. An interesting alternative to the ground-state destabilization mechanism has been proposed by Harris *et al.*,[10] who suggest that a very short hydrogen bond may form between Asp70 and the substrate carboxylate.

Warshel *et al.*[17] have recently used a combination of *ab initio* quantum mechanical calculations, empirical valence bond (EVB) simulations, and free-energy perturbation (FEP) calculations to demonstrate that the catalytic effect of ODCase is due to transition-state stabilization rather than ground-state destabilization. They argue that the Wu *et al.* proposal,[16] which involves ground-state destabilization due to repulsion between the substrate carboxylate and the anionic form of Asp70, is problematic since the destabilized substrate (or Asp70) will accept a proton from the solvent and form a new stable ground state. Furthermore, they alert us to the fact that the extremely large binding energy (−26 kcal/mol) that was computed by Wu *et al.*[16] for the phosphoribosyl region of the substrate has no precedent and is inconsistent with recent experiments by Miller *et al.*,[12,53] who found that the region contributed only ∼5 kcal/mol to stabilizing the transition-state analogue, 6-hydroxyuridine 5′-phosphate (BMP). Warshel *et al.*[17] studied the reaction with the substrate carboxylate in its ionized form and with the neighboring protein groups in their ionized forms. They observed that this configuration does not lead to ground-state destabilization. Their results reveal that the transition state is preferentially stabilized relative to the ground state, which is found to be stabilized to a small extent rather than destabilized. Upon transfer from the ground state to the transition state, there is a significant increase in the dipole moment of the reacting system since the charge separation is greater between the positively charged Lys72 and the negative charge on C6 of the substrate than between Lys72 and the substrate carboxylate. They conclude that the transition-state stabilization arises from the fact that the enzyme has preorganized the active site environment of the ground state in a configuration that contains electrostatic stress between Asp70 and Asp75B, but is complementary to the significantly larger dipole moment of the transition-state ion pair.[17,18]

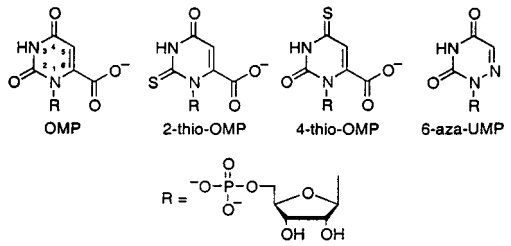

Figure 1. Ligands used in this study.

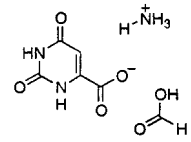

Figure 2. Final model system used in the quantum calculations.

We also find the notion of "ground-state destabilization" counterintuitive. Here, we present an alternative mechanism that explains the remarkable catalytic efficiency of ODCase. The mechanism involves equilibrium pre-protonation of C5 of OMP by Lys72 followed by decarboxylation, where Asp70 is in its neutral form. This protonation state of Asp70 is in contrast to that reported by Warshel *et al.*,[17] who claimed that their pK_a calculations find Asp70 to be anionic, but did not report the computed value. Our proposed mechanism is supported by QM-FE (quantum mechanical-free energy) calculations on the enzymatic reaction,[19,20] molecular dynamics (MD) simulations of the enzyme in complexes with various ligands, pictured in Figure 1, pK_a calculations, and free energy calculations using the MM-PBSA approach of Srinivasan *et al.*[21] The mechanism is also consistent with available kinetic isotope effect experimental data on this enzyme.

2. Methods

2.1. QM Calculations on Model Systems. Reaction energy profiles for C5- and C6-protonation of the substrate by Lys72 were calculated using a model system consisting of three species: orotate, ammonium ion, and a neutral formic acid (Figure 2). The coordinates for these species were taken from the corresponding molecules in the crystal structure. Justification for representing Asp70 in its neutral form as opposed to its anionic form is presented under Discussion and Conclusions. Each reaction energy profile was obtained by constraining the distance between the nearest hydrogen atom of the ammonium ion and the C5 atom or the C6 atom of the orotate ring. The constraint was done through fixing the corresponding internal coordinate in the Gaussian 98 input file, which is equivalent to a harmonic restraining force with infinite force constant. For each point along the reaction coordinate, all geometric parameters except for the constrained distance

(14) Smiley, J.; Jones, M. *Biochemistry* **1992**, *31*, 12162−12168.
(15) Houk, K. N.; Lee, J. K.; Tantillo, D. J.; Bahmanyar, S.; Hietbrink, B. N. *ChemBioChem* **2001**, *2*, 113−118.
(16) Wu, N.; Christendat, D.; Dharamsi, A.; Pai, E. *Acta Crystallogr. D* **2000**, *56*, 912−914.
(17) Warshel, A.; Strajbl, M.; Villa, J.; Florian, J. *Biochemistry* **2000**, *39*, 14728−14738.
(18) Warshel, A.; Florián, J.; Strajbl, M.; Villà, J. *ChemBioChem* **2001**, *2*, 109−111.
(19) Stanton, R.; Perakyla, M.; Bakowies, D.; Kollman, P. *J. Am. Chem. Soc.* **1998**, *120*, 3448−3457.
(20) Kuhn, B.; Kollman, P. *J. Am. Chem. Soc.* **2000**, *122*, 2586−2596.
(21) Srinivasan, J.; Cheatham, T.; Cieplak, P.; Kollman, P.; Case, D. *J. Am. Chem. Soc.* **1998**, *120* , 9401−9409.

were optimized at the HF/6-31+G* level; single-point energies were calculated at both the HF/6-31+G* and MP2/6-31+G* levels. Reaction energy profiles for the decarboxylations of orotate and the C5-protonated intermediate were calculated at the same levels of theory. Single-point energies for the C5-protonation reaction profile as well as that for decarboxylation of the C5-protonated intermediate were also calculated at the MP2/cc-pVDZ level. In some cases, solvation effects were calculated using the PCM model within the Gaussian 98 package.[22] Gas-phase proton affinities (PAs) were computed by calculating the energy difference between the protonated and unprotonated species at the MP2/6-31+G*//HF/6-31+G* level. Equilibrium isotope effects (EIEs) for the C5-protonation step were determined by obtaining the ratio of fractionation factors for the orotate and the corresponding C5-protonated intermediate ($\phi_{\text{orotate}}/\phi_{\text{intermediate}}$). Fractionation factors at 298 K were computed by using the Bigeleisen equation[23] implementation via the QUIVER program,[24] which employs the Cartesian force constant matrices for the respective states as input. The matrices were obtained using the Gaussian 98 package[22] at the HF/6-31+G*//HF/6-31+G* level and scaled by the default value of 0.8929. Unless otherwise noted, all of the above calculations were performed using the Gaussian 98 package[22] on the Origin 2000 cluster at the National Center for Supercomputing Applications (NCSA) at the University of Illinois at Urbana−Champaign and the Cray SV1 cluster at the National Cancer Institute (NCI).

2.2. QM-FE Calculations. Combined quantum mechanical and free energy (QM-FE)[19,20] calculations were performed to incorporate the effect of the enzyme environment on the reaction energy profile for C5-protonation. This approach has also been used by Jorgensen on many organic reactions.[25−27] The overall free energy change, ΔG^*, for C5-protonation in the enzyme is approximated as

$$\Delta G^* = \Delta E_{\text{QM}} + \Delta G_{\text{FE}} \quad (1)$$

where ΔE_{QM} is the quantum mechanical (QM) energy difference and ΔG_{FE} the molecular mechanical (MM) free energy difference between the reactants and the C5-protonated intermediate. The QM region was defined as the orotate ring and the methylammonium ion (representing Lys72), the only parts of the system that undergo bond cleavage and formation. The MM region was defined as the rest of the substrate and protein. Link atoms consisted of the C1 atom of orotate and the Cδ atom of Lys72, which were treated as hydrogens in the QM calculations, but as carbons in the MM free energy calculations. It is critical that parts of the system included in the QM region are not included in the MM region to avoid double counting. The neighboring charged residues of Lys72 (Lys42, Asp70, Asp75B) were assigned to the MM region due to the fact that including these residues in the QM *in vacuo* calculation would have greatly exaggerated their effect on the C5-protonation barrier compared to their influence in the higher dielectric environment of the enzyme. QM energies were taken from calculations on model systems (see QM results section, below). Charges for the QM region were obtained by a restrained electrostatic potential fitting method (RESP)[28] with the following modifications: the C1 atom charge, which was near zero and fluctuated slightly over different stages of the free energy calculation, was set to zero to avoid unphysical effects on the overall free energy change. The charge of the Cδ atom of Lys72 was taken from that of the corresponding hydrogen in the QM region. The thermodynamic integration (TI)[29] method with 101 equally spaced windows for each direction was employed for the free energy calculations, using the MD protocol described above with different nonbonded cutoffs to study the influence of the nonbonded cutoff on the computed ΔG_{FE}. Various total simulation lengths ranging from 10 to 80 ps were performed. During each simulation, one hydrogen attached to the Lys72 nitrogen "disappeared" gradually and became a dummy atom, while a dummy atom attached to the orotate C5 atom slowly became a hydrogen atom. This manner of performing the simulation obviates the need to consider the pathway for proton transfer from Lys72 to the orotate ring. Since other energy terms are already included in the QM energies, the MM free energies consist of only van der Waals and electrostatic interactions between the QM and MM regions that are extracted from the simulation, as has been done by Stanton *et al.*[19] and Kuhn *et al.*[20]

2.3. Molecular Dynamics (MD) Simulations. Coordinates for the ODCase dimer were extracted from monomers C and D in the 1.5-Å-resolution crystal structure of the *Methanobacterium thermoautotrophicum* enzyme in complex with the 6-azauridine 5′-phosphate (6-aza-UMP) inhibitor (1DVJ in the Protein Data Bank).[13] The ligand in the active site of monomer C was included in the model, while the active site of monomer D was left empty. Even though the active species of the enzyme is a dimer, it has been shown that the monomers are catalytically independent, such that the E_2S_2 complex can be treated as E_2S.[30] All residues (9−222) of monomers C and D were included in the model with the exception of the cloning artifact and missing residues distant from the active site. Acetyl and *N*-methyl capping groups were added to the N-terminal and C-terminal truncated ends, respectively, using the LEaP module in the AMBER 5.0 package.[31] In the same module, hydrogen atoms were added, and all histidines were protonated by default at the δ-nitrogen. As described above, Asp70 in the ligand-bound active site was assigned to be neutral for all the enzyme−ligand complexes unless otherwise noted. Ionization states present in neutral solution were used for all other charged residues. All crystallographic waters within 35 Å of the Nζ atom of Lys72 in monomer C were included, yielding a total of 316 waters. Each system was solvated by placing a spherical cap of TIP3P water molecules[32] with a radius of 35 Å centered at the Nζ atom of Lys72 in monomer C. Neutralizing counterions were added within the LEaP module. Coordinates for the substrate (OMP) and its thio-substituted analogues (2-thio-OMP and 4-thio-OMP) were obtained by modifying the 6-aza-UMP ligand in the LEaP module of the AMBER 5.0 package.[31] Based on the free energy reaction profile computed by Wu *et al.*,[13] a "transition-state" ligand was defined as having the same geometry as the substrate, but with a bond of 2.4 Å between C6 and the carboxyl carbon. This structure was optimized at the 6-31+G* level with the C6−CO_2^- bond constrained to 2.4 Å. Ligand bond, angle, and dihedral parameters not present in the Cornell *et al.* force field[33] are listed in the Supporting Information. Charges for the ligands and transition-state model were obtained by the RESP method.[28] Phosphoribosyl and base fragments were defined by splitting the ligand at the C1*−N1 bond and capping with formamide and methyl groups, respectively. Electrostatic potentials for these fragments were then derived from HF/6-31+G*//HF/6-31+G*

(22) Frisch, M. J.; Trucks, G. W.; Schlegel, H. B.; Scuseria, G. E.; Robb, M. A.; Cheeseman, J. R.; Zakrzewski, V. G.; Montgomery, J. A., Jr.; Stratmann, R. E.; Burant, J. C.; Dapprich, S.; Millam, J. M.; Daniels, A. D.; Kudin, K. N.; Strain, M. C.; Farkas, O.; Tomasi, J.; Barone, V.; Cossi, M.; Cammi, R.; Mennucci, B.; Pomelli, C.; Adamo, C.; Clifford, S.; Ochterski, J.; Petersson, G. A.; Ayala, P. Y.; Cui, Q.; Morokuma, K.; Malick, D. K.; Rabuck, A. D.; Raghavachari, K.; Foresman, J. B.; Cioslowski, J.; Ortiz, J. V.; Stefanov, B. B.; Liu, G.; Liashenko, A.; Piskorz, P.; Komaromi, I.; Gomperts, R.; Martin, R. L.; Fox, D. J.; Keith, T.; Al-Laham, M. A.; Peng, C. Y.; Nanayakkara, A.; Gonzalez, C.; Challacombe, M.; Gill, P. M. W.; Johnson, B. G.; Chen, W.; Wong, M. W.; Andres, J. L.; Head-Gordon, M.; Replogle, E. S.; Pople, J. A. *Gaussian 98*, revision A.6; Gaussian, Inc.: Pittsburgh, PA, 1998.

(23) Bigeleisen, J.; Goeppert-Mayer, M. *J. Chem. Phys.* **1947**, *15*, 261−267.

(24) Saunders, M.; Laidig, K.; Wolfsberg, M. *J. Am. Chem. Soc.* **1989**, *111*, 8989−8994.

(25) Chandrasekhar, J.; Smith, S.; Jorgensen, W. *J. Am. Chem. Soc.* **1985**, *107*, 154−162.

(26) Chandrsekhar, J.; Jorgensen, W. *J. Am. Chem. Soc.* **1985**, *107*, 2974−2975.

(27) Severance, D.; Jorgensen, W. *ACS Symp. Ser.* **1993**, *568*, 243−259.

(28) Bayly, C.; Cieplak, P.; Cornell, W.; Kollman, P. *J. Phys. Chem.* **1993**, *97*, 10269−10280.

(29) Beveridge, D.; DiCapua, F. *Annu. Rev. Biophys. Biophys.* **1989**, *18*, 431−492.

(30) Porter, D.; Short, S. *Biochemistry* **2000**, *39*, 11788−11800.

(31) Case, D.; Pearlman, D.; Caldwell, J.; Ross, W.; Cheatham, T., III; Ross, W.; Simmerling, C.; Darden, T.; Merz, K.; Stanton, R.; Cheng, A.; Vincent, J.; Corwley, M.; Ferguson, D.; Radmer, R.; Seibel, G.; Singh, U.; Weiner, P.; Kollman, P. *Amber 5.0*; University of California, San Francisco, CA, 1997.

(32) Jorgensen, W.; Chandrasekhar, J.; Madura, J.; Impey, R.; Klein, M. *J. Chem. Phys.* **1983**, *79*, 926−935.

(33) Cornell, W.; Cieplak, P.; Bayly, C.; Gould, I.; Merz, K.; Ferguson, D.; Spellmeyer, D.; Fox, T.; Caldwell, J.; Kollman, P. *J. Am. Chem. Soc.* **1995**, *117*, 5179−5197.

QM calculations using the Gaussian 98 package.[22] Charges were obtained by fitting each fragment independently such that the net charge of the phosphoribosyl fragment was −2 and that of the base fragment was −1 (for OMP, 2-thio-OMP, and 4-thio-OMP) or 0 (for 6-aza-UMP); the capping groups were constrained to have zero net charge. For OMP, good agreement was found between the charges obtained in this manner and those obtained by using the entire molecule for deriving the electrostatic potentials. Independent treatment of the phosphoribosyl and base fragments is therefore valid for all the ligands in this study.

Molecular dynamics simulations were performed using the Cornell *et al.* force field[33] and the AMBER 5.0 suite of programs.[31] The SHAKE algorithm was applied to constrain all bonds to their equilibrium values.[34] A 12-Å residue-based cutoff was used for nonbonded interactions. Only residues (including ions, water molecules, and the ligand) that lie in the "belly", the region within 18 Å of the Nζ atom of Lys72, were allowed to move. Minimization and equilibration were performed in two stages. In the first stage, ions in the belly and all water molecules were minimized for 10 cycles of steepest descent followed by 990 cycles of conjugate gradient, and then equilibrated for 10 ps while the temperature was raised from 0 to 300 K. In the second stage, the entire belly region was minimized in the same manner, and then equilibrated for 60 ps while the temperature was raised from 0 to 300 K. Sampling of reasonable configurations for the given stable state of the enzyme−ligand structure was conducted by running a 300-ps belly simulation with a 2-fs time step at 300 K. Constant temperature was maintained by the Berendsen coupling algorithm[35] with separate solute−solvent and solvent−solvent coupling. The equilibrated coordinates and velocities of the enzyme−OMP complex were used as the starting points for the simulations of the enzyme−(2-thio-OMP) and the enzyme−(4-thio-OMP) complexes.

2.4. MM-PBSA Calculations. To compute the average binding free energy of each enzyme−ligand complex, we sampled 15 equally spaced "snapshot" configurations of the unbound enzyme, unbound ligand, and enzyme−ligand complex from the last 150 ps of the complex trajectory and performed energy calculations on the snapshots. Prior to the energy calculations, all waters and ions were removed from each snapshot. Free energy calculations were performed using the MM-PBSA approach, described in detail by Srinivasan *et al.*[21] The binding free energy, ΔG_{bind}, is defined as follows:

$$\Delta G_{\text{bind}} = \langle \Delta E_{\text{MM}} \rangle + \Delta G_{\text{solv}} - T\Delta S \tag{2}$$

$$\langle \Delta E_{\text{MM}} \rangle = \langle \Delta E_{\text{elec}} \rangle + \langle \Delta E_{\text{vdW}} \rangle + \langle \Delta E_{\text{int}} \rangle$$

$$\Delta G_{\text{solv}} = \Delta G_{\text{PB}} + \Delta G_{\text{SA}}$$

where $\langle \Delta E_{\text{MM}} \rangle$ is the change in the total MM energy of the solute with an electrostatic component ($\langle \Delta E_{\text{elec}} \rangle$), a van der Waals component ($\langle \Delta E_{\text{vdW}} \rangle$), and an internal component ($\langle \Delta E_{\text{int}} \rangle$) consisting of bond, angle, and torsional energies; ΔG_{solv} is the solvation energy difference, which consists of an electrostatic contribution (ΔG_{PB}) determined by the Poisson−Boltzmann approach using the DelPhi2.0 software package[36] and a nonelectrostatic contribution (ΔG_{SA}) that is linearly dependent on the surface area; and $-T\Delta S$ is the solute entropic contribution to the binding free energy. Solute entropic contributions were not calculated in this study since they are only crudely estimated by normal-mode analysis and likely to be similar for all the enzyme−ligand complexes. Because the same enzyme and ligand configurations are used for their respective unbound and bound states, $\langle \Delta E_{\text{int}} \rangle$ is equal to zero. Calculations of both the electrostatic component to the MM energy and the electrostatic contribution to the solvation energy were performed using two different solute, or "interior", dielectric (ϵ_{int}) values, 1 and 4.

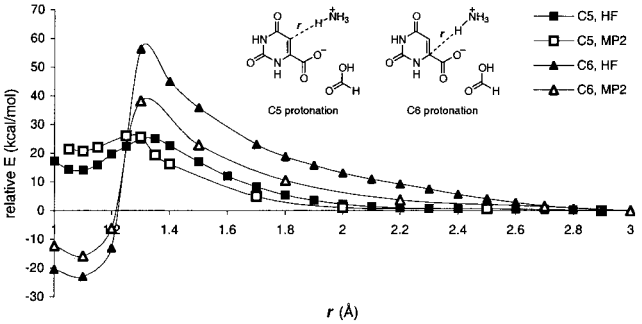

Figure 3. Energy profiles for the C5- and C6-protonations of orotate by an ammonium ion with a formic acid hydrogen bonded to the orotate carboxyl group at the HF/6-31+G*//HF/6-31+G* and MP2/6-31+G*//HF/6-31+G* levels.

The pK_a value of Asp70 in the enzyme−substrate complex was calculated using a new methodology developed by B. Kuhn in our laboratory (B. Kuhn, unpublished results). This method employs the MM-GBSA approach in which generalized Born/surface area (GBSA) calculations are performed instead of the Poisson−Boltzmann and surface area calculations that are described above. The pK_a of a selected residue is defined as follows:

$$\text{p}K_a = \text{p}K_a^{\text{sol}} + \Delta\Delta G^{\text{deprot}}/RT \ln 10 \tag{3}$$

where $\text{p}K_a^{\text{sol}}$ is the pK_a of the residue free in neutral solution, $\Delta\Delta G^{\text{deprot}}$ is the energy of deprotonating the residue in the enzyme−substrate complex ($\Delta G^{\text{complex}}$) relative to that of deprotonating the residue when it is free in solution (ΔG^{sol}), R is the ideal gas constant, and T is the temperature. The alternative protonation state of Asp70 was modeled into 20 selected configurations from the trajectory of the enzyme−substrate complex (or Asp70 free in solution capped by acetyl and *N*-methyl groups). Free energies of the anionic and neutral Asp were obtained by minimizing Asp70 in the relevant environment and calculating the GBSA energy[37] using parameters from Jayaram *et al.*[38] and a nonbonded cutoff of 25 Å in the AMBER 6.0 suite of programs.[39] Both tautomers of the neutral Asp were taken into consideration, and the preferred protonation site was chosen on the basis of the lower free energy. All GBSA calculations were done using $\epsilon_{\text{int}} = 4$.

3. Results

3.1. QM and QM-FE Calculations. 3.1.1. Energy Profile of C5 Protonation and C6 Protonation. As shown in Figure 3, the barrier for C5-protonation is significantly lower than that of C6-protonation when the energy profiles are calculated at either the HF/6-31+G*//HF/6-31+G* or the MP2/6-31+G*//HF/6-31+G* level. Furthermore, C5-protonation appeared more consistent with the experimental evidence for a stepwise mechanism[5] since it yielded an intermediate while C6-protonation proceeded directly to decarboxylation. We therefore focused on the C5-protonation mechanism.

To obtain geometries for the ammonium−orotate attack that are less distorted by the attraction between the ammonium and the substrate carboxylate, the C5-protonation energy profile was computed without formic acid, using the geometries optimized in the presence of formic acid. The results of this calculation are shown in Figure 4. From this result and the result in Figure 3, the formic acid appears to keep the orotate carboxyl group

(34) Ryckaert, J.; Ciccotti, G.; Berendsen, H. *J. Comput. Phys.* **1977**, *23*, 327−341.
(35) Berendsen, H.; Postma, J.; van Gunsteren, W.; DiNola, A.; Haak, J. *J. Comput. Phys.* **1984**, *81*, 3684−3690.
(36) Sharp, K.; Honig, B. *Annu. Rev. Biophys. Biophys.* **1990**, *19*, 301−332.
(37) Weiser, J.; Shenkin, P.; Still, W. *J. Comput. Chem.* **1999**, *20*, 217−230.
(38) Jayaram, B.; Sprous, D.; Beveridge, D. *J. Phys. Chem. B* **1998**, *102*, 9571−9576.
(39) Case, D.; Pearlman, D.; Caldwell, J.; Cheatham, T., III; Ross, W.; Simmerling, C.; Darden, T.; Merz, K.; Stanton, R.; Cheng, A.; Vincent, J.; Crowley, M.; Tsui, V.; Radmer, R.; Duan, Y.; Pitera, J.; Massova, I.; Seibel, G.; Singh, U.; Weiner, P.; Kollman, P. *Amber 6.0*; University of California, San Francisco, CA, 1999.

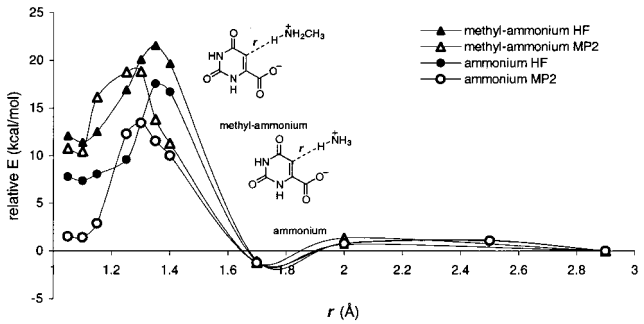

Figure 4. Energy profiles for C5-protonation of orotate by ammonium ion with geometries taken from Figure 3 and energies calculated at the HF/6-31+G* and MP2/6-31+G* levels. Profiles for C5-protonation by methylammonium ion are also shown.

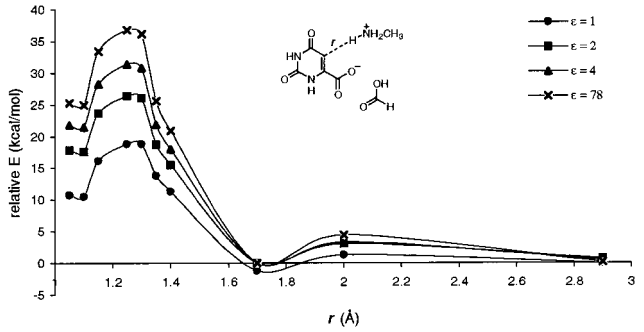

Figure 5. Energy profile for the C5-protonation of orotate by a methylammonium ion with geometries taken from Figure 3. The geometry of the methyl group was optimized at the HF/6-31+G* level with the COSMO continuum solvent model using different dielectric constants. Energies were calculated at the HF/6-31+G* and MP2/6-31+G* levels.

from being distorted due to hydrogen bonding with the ammonium ion, rather than stabilizing the reaction through electronic effects. To more accurately represent Lys72 in the enzyme, the ammonium hydrogen corresponding to the Cξ position of Lys72 was replaced with a methyl group, important because methylamine has a greater proton affinity than NH_3. The energy barrier to C5-protonation by methylamine is ~18 kcal/mol, while the energy difference between the reactants and the intermediate is ~10 kcal/mol (Figure 4). Use of a larger basis set lowers these values to ~13 and ~9 kcal/mol, respectively, as determined at the MP2/cc-pVDZ level of theory. Thio substitutions at the 2 and 4 positions on the orotate ring caused changes of less than 1 kcal/mol on both energy barriers and relative energies (data not shown).

The effect of the enzyme environment on the C5-protonation is challenging to estimate since there are several charged groups in the active site region. To examine the sensitivity of the protonation barrier to the polarizability of the enzyme environment, the PCM continuum solvent model was used with a range of dielectric constant values (ϵ) of 2, 4, and 80. Results are shown in Figure 5. The effect of the continuum model is to increase both the energy barrier and the relative energy. With $\epsilon = 2$, the energy barrier becomes ~26 kcal/mol and the relative energy ~17 kcal/mol. With $\epsilon = 4$ or 80, the corresponding barriers are even larger. However, the use of continuum models in this way has been appropriately criticized.[17,40,41] Such models, when used without explicit representation of the many charged residues near the orotate moiety, are unlikely to accurately reproduce the energetics of proton transfer.

Table 1. Average MM Free Energy Differences[a] (in kcal/mol) for the C5-Protonated Intermediate Relative to the Ground State Determined by QM-FE Calculations for Different Simulation Lengths and Nonbonded Cutoffs

	8 Å	10 Å	12 Å
10 ps	-18.3 ± 6.0	-10.2 ± 6.6	-15.2 ± 2.3
20 ps	-11.9 ± 7.4	-41.5 ± 17.5	-33.4 ± 2.6
40 ps	-41.4 ± 6.7	-32.9 ± 7.7	-41.2 ± 3.4
80 ps	-16.3 ± 1.9	-27.7 ± 17.8	-15.1 ± 4.9

[a] Averages are from backward and forward simulations with the range given, e.g., -20 ± 10 means one simulation leads to a free energy of -30 kcal/mol, the other, -10 kcal/mol.

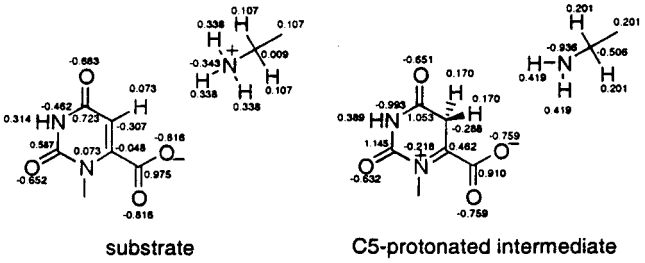

Figure 6. Partial charges for the QM atoms in the ground and C5-protonated intermediate states used in the QM-FE calculations.

To more realistically account for the enzyme environment, QM-FE calculations[19,20] were performed on this system to estimate the energy of the C5-protonated intermediate relative to the ground state. This methodology, which involves treating only the minimal part of the system with *ab initio* quantum mechanics and representing the rest with molecular mechanics, has been reviewed by Kollman *et al.*[42] and has accurately determined the $\Delta G^{\ddagger}$ for three other enzymes.[19,20,43] Warshel[44] has had success with a similar approach involving EVB simulations. As described in the Methods section, the overall free energy change (ΔG^*) for C5-protonation is approximated as the sum of the difference in QM energy (ΔE_{QM}) and the difference in the free energy of interaction (ΔG_{FE}). The above calculations have shown that ΔE_{QM} is ~10 kcal/mol. To be consistent with the experimental k_{cat} and the fact that decarboxylation is the rate-limiting step would require the stabilizing effect of the enzyme environment (ΔG_{FE}) to be less than -5 kcal/mol. The average differences in the free energy of interaction (ΔG_{FE}) are presented in Table 1, and the charge distributions of the QM atoms in the ground and intermediate states are shown in Figure 6. Although the computed stabilization of the C5-protonated intermediate is unrealistically more negative than -5 kcal/mol and still fluctuating as a function of nonbonded cutoff and simulation length, the qualitative result shows consistently that the enzyme stabilizes the intermediate relative to the reactants. Given the large uncertainty in the electrostatic energy with the numerous charged groups in the substrate and nearby residues, free energy calculations with particle mesh Ewald[43] would need to be performed to accurately calculate the energy of the intermediate relative to the ground state. However, this system is large for full periodic box MD-FE simulations and, with the large number of charges in the active site, would require very long calculations for quantitative convergence. We also note that the gas-phase barrier to C5-protonation at the MP2/6-31+G* level (Figure 4) is

(40) Warshel, A. *J. Biol. Chem.* **1998**, *273*, 27035−27038.
(41) Warshel, A.; Florian, J. *Proc. Natl. Acad. Sci. U.S.A.* **1998**, *95*, 5950−5955.
(42) Kollman, P.; Kuhn, B.; Donini, O.; Perakyla, M.; Stanton, R.; Bakowies, D. *Acc. Chem. Res.* **2001**, *34*, 72−79.
(43) Donini, O.; Darden, T.; Kollman, P. *J. Am. Chem. Soc.* **2000**, *122*, 12270−12280.
(44) Warshel, A. *Computer Modeling of Chemical Reactions in Enzymes and Solutions*; Wiley: New York, 1991.

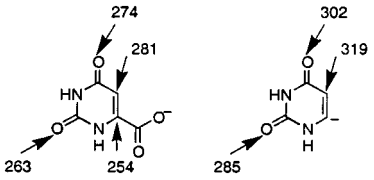

Figure 7. Calculated gas-phase proton affinity for different sites of orotate and deprotonated uracil in kilocalories per mole at the MP2/6-31+G*//HF/6-31+G* level.

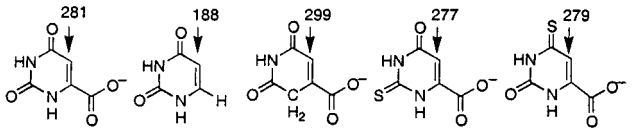

Figure 8. Calculated gas-phase proton affinity for different derivatives of orotate in kilocalories per mole at the MP2/6-31+G*//HF/6-31+G* level.

~18 kcal/mol and that some of the environmental stabilization of the protonated intermediate is likely to occur at the transition state for protonation. It could well be that the transition state in Figure 4 is stabilized by a significant fraction of the −5 to −10 kcal/mol stabilization that is experienced by the C5-protonated intermediate. The goal here is not to attain a quantitative ΔG^*, but to show that the enzyme environment stabilizes the C5-protonated intermediate over the reactant of an order of magnitude such that $\Delta G^* = \Delta E_{QM} + \Delta G_{FE}$ is significantly less than the ΔE_{QM} (Figure 4, ~10 kcal/mol), in contrast to what is suggested by the continuum calculations, Figure 5, where a general environmental effect destabilizes the protonated intermediate.

3.1.2. Proton Affinities. The calculated gas-phase proton affinities (PA) of different sites of orotate and deprotonated uracil are shown in Figure 7. Since the addition of a proton to C6 will result in decarboxylation, the PA of C6 was calculated by constraining the C6−H distance at 1.09 Å and the C6−carboxyl carbon distance at 1.60 Å; these values are taken from the equilibrium distances of C5-protonated orotate. Lee and Houk[4] compared the PAs of O2 and O4 positions of orotate and concluded that O4 is the preferred protonation site. Surprisingly, the PA of C5 is higher than that of either O2 or O4, both in orotate and in deprotonated uracil. These results show that C5 is intrinsically more basic than O2, O4, or C6.

PAs for some derivatives of orotate were also computed (Figure 8). The fact that the PA of C5 is nearly 100 kcal/mol lower in uracil than in orotate indicates that the carboxylate group plays a critical role in raising the PA of C5. The C5 PA of both the 2-thio and 4-thio substrate analogues is similar to that of the unsubstituted substrate, suggesting that these substitutions do not have a large effect on the electronic structure near the C5 position. The fact that the proton affinity increases upon replacing the N1−H by CH_2 suggests that there is little or no stabilization of protonation at C5 by resonance delocalization effects due to N1.

3.1.3. Energy Profile of Decarboxylation. As shown in Figure 9, the barrier to decarboxylation of orotate is 35−40 kcal/mol, in accord with experimental results[1] and other computational results[4,13] for the nonenzymatic reaction. This barrier is greatly reduced to ~10 kcal/mol for the C5-protonated intermediate (Figure 9). At the MP2/cc-pVDZ level, the same barrier is reduced to ~5 kcal/mol. Incorporation of environmental effects using the PCM model increases this barrier to 10, 15, and 21 kcal/mol using dielectric constant values of 2, 4, and 80, respectively. Barriers to decarboxylation for the 2-thio and 4-thio substrate analogues (data not shown) are within 1 kcal/mol of that of the unsubstituted substrate.

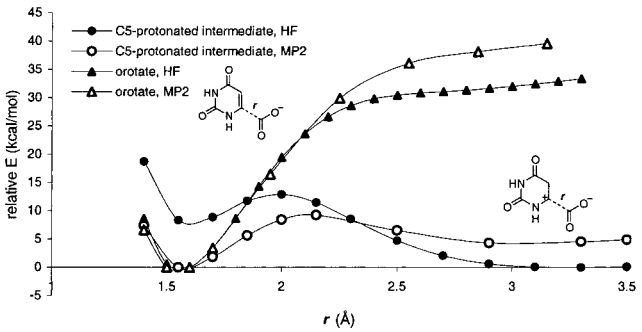

Figure 9. Energy profiles for the decarboxylation of orotate and of the C5-protonated intermediate at the HF/6-31+G*//HF/6-31+G* and MP2/6-31+G*//HF/6-31+G* levels.

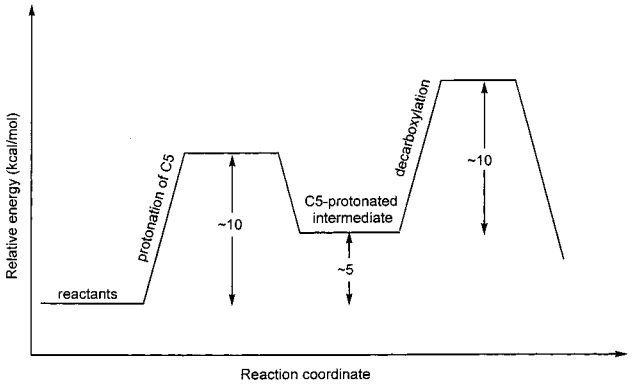

Figure 10. Qualitative energy profile illustrating the plausibility of the proposed mechanism of catalysis by ODCase. The forward barrier height of decarboxylation of the C5-protonated intermediate was computed by gas-phase *ab initio* QM calculations at the MP2/6-31+G*//HF/6-31+G* level (Figure 9). The energy of the C5-protonated intermediate relative to reactants ($\Delta G^* = \Delta E_{QM} + \Delta G_{FE}$) was estimated from QM-FE calculations, which yielded a QM energy difference (ΔE_{QM}) of ~10 kcal/mol (Figure 4) at the MPS/6-31+G* //HF/6-31+G* level for C5-protonation by methylammonium ion and a stabilizing effect of the enzyme environment (ΔG_{FE}) that is unrealistically favorable as well as not converged due to inaccurate treatment of long-range electrostatics (Table 1). Given that decarboxylation is the rate-limiting step and that the experimental $\Delta G^{\ddagger}$ is 15 kcal/mol,[1] the stabilizing effect of the enzyme environment would be expected to be less than −5 kcal/mol, such that the relative energy of the intermediate to reactants is 5 kcal/mol as shown. A significant fraction of the −5 to −10 kcal/mol environmental stabilization of the protonated intermediate is likely to be experienced by the transition state of the protonation step such that the computed barrier of ~18 kcal/mol at the MP2/6-31+G*//HF/6-31+G* level is reduced to an estimate of ~10 kcal/mol.

Combining the results from the QM calculations of both protonation and decarboxylation and our less rigorously derived, but plausible, estimates for the free energy of environmental stabilization for the protonation step, we suggest a free energy profile for the reaction as shown in Figure 10. As noted above, our free energy calculations lead to an unrealistically large stabilization of the protonated intermediate by −11 to −40 kcal/mol, but using ~10 kcal/mol for the QM barrier to protonation and an environmental stabilization of ~ −5 kcal/mol leads to the illustrated barrier and relative energy for the C5-protonated intermediate. For the decarboxylation step, the QM calculations suggest a barrier of ~10 kcal/mol (MP2/6-31+G*) and ~5 kcal/mol (MP2/cc-pVDZ), with continuum solvation raising this value by 5−16 kcal/mol (ϵ values of 2−80). Free energy

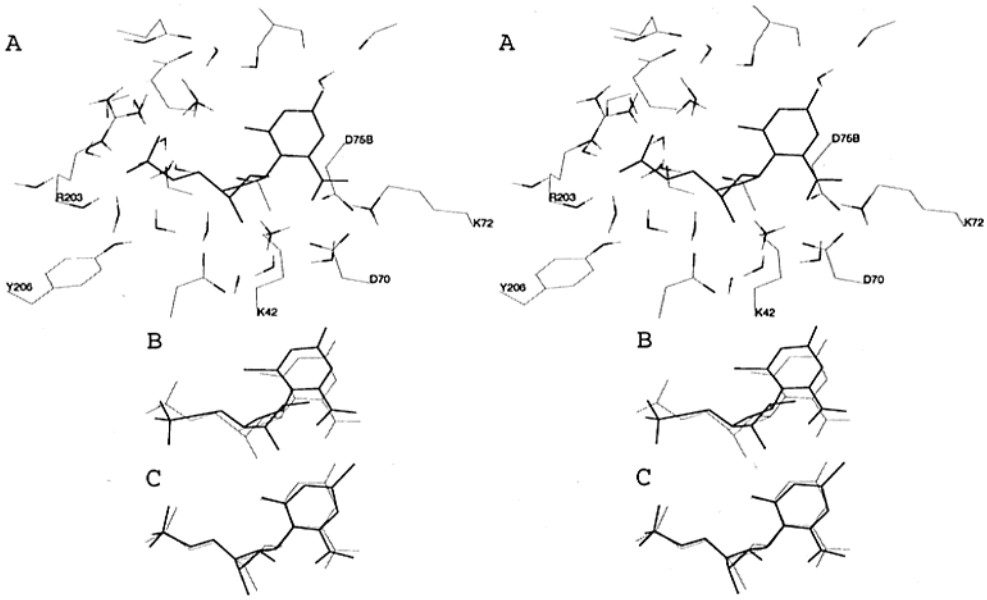

Figure 11. Stereoviews of final structures from MD trajectories. (A) Active site residues (gray) and OMP (black); (B) 4-thio-OMP (black) superimposed onto OMP (gray) using a least-squares fit of the residues hydrogen bonding to OMP; and (C) 2-thio-OMP (black) superimposed onto OMP (gray) using the same method. Produced with the MidasPlus graphics program.[54]

perturbation calculations on this step would be desirable but are likely to suffer from the same uncertainty in the electrostatic energy as observed in the QM-FE calculations on the protonation step. All we can claim is that the barrier to decarboxylation of the C5-protonated intermediate is much smaller than that of orotate and that our calculated values (5−21 kcal/mol) are in the range consistent with the experimental $\Delta G^{\ddagger}$ of orotate. The rate-limiting step is therefore the decarboxylation with a net $\Delta G^{\ddagger}$ of ∼15 kcal/mol relative to reactants. The protonated intermediate is less stable than reactants by ∼5 kcal/mol, but the barrier to achieve it is significantly less than 15 kcal/mol, such that the decarboxylation is clearly rate-limiting. This reaction profile is consistent with the finding by Ehrlich *et al.*[5] that the protonated intermediate deprotonates with greater probability than proceeding through decarboxylation.

3.2. MD. Stable dynamics of all the enzyme−ligand complexes were obtained from the simulation protocol and force field parameters as indicated by low belly atom root-mean-square deviations (RMSD) from the average structure. For the enzyme−(6-aza-UMP) complex, the RMSD of the belly atoms from the average structure ranged from 0.3 to 0.4 Å, while the RMSD from the minimized crystal structure remained steady at 0.6 Å over the entire 300 ps trajectory. As the other ligands were constructed from the 6-aza-UMP complex crystal structure, the first 150 ps were omitted from analysis to allow for additional equilibration. This equilibration period was sufficient for all cases except for the 2-thio-OMP complex trajectory, in which considerable RMSD fluctuations occurred in the 150−300 ps interval. This trajectory was therefore extended to 1 ns. The belly atom RMSDs from the average structures over the final 150 ps of the substrate, 4-thio-OMP, and extended 2-thio-OMP complex trajectories ranged from 0.3 to 0.6 Å.

To explore the feasibility of the C5-protonation mechanism, key interatomic distances were computed. Specifically, it was noted that neutral Asp70 forms a hydrogen bond with the substrate carboxylate throughout the complex trajectory. Furthermore, Lys72 lies out of the plane of the orotate ring with the distance between the Nζ atom of Lys72 and C5 in the substrate (OMP) fluctuating between 3.4 and 5.2 Å. The proximity of these two atoms at various points of the trajectory makes it possible for Lys72 to donate a proton to C5 of the substrate. Thus, the dynamics of the enzyme−substrate complex are consistent with the proposed C5-protonation mechanism.

The dynamics of the 4-thio-OMP and 2-thio-OMP complexes are also consistent with experimental kinetics data. Shostak and Jones observed no enzyme activity for the 2-thio-OMP ligand, while the reaction rate was only slightly diminished for the 4-thio-OMP ligand (50% reduction in k_{cat}).[8] Since the experimental binding free energies of these thio-substituted ligands are similar to that of the natural substrate, subtle differences in the dynamics of the 2-thio-OMP complex are likely to be responsible for the dramatic decrease in catalytic activity. To examine differences in the dynamics of the substrate, 4-thio-OMP, and 2-thio-OMP complexes, the latter two were superimposed onto the substrate through least-squares fits of the active site residues pictured in Figure 11A. As pictured in Figure 11B,C, the position of the orotate ring in 2-thio-OMP has shifted, and its phosphoribosyl portion has changed in conformation from that of the substrate while the position of 4-thio-OMP is similar to that of the substrate. As the 2-carbonyl in the substrate participates in a water-mediated hydrogen bond to Gln185, its replacement with a thiocarbonyl likely causes a disruption in the network of hydrogen bonds. This disruption somehow leads to a loss in catalytic activity.

Since protonation of C5 of the ligand by Lys72 is key in our proposed mechanism, it was predicted that Lys72 would be positioned close to C5 for only a small percentage of the time, if at all, during the 2-thio-OMP complex trajectory. Table 2 shows the statistical data on the distances between Nζ of Lys72 and C5 of the ligand as sampled by the substrate, 4-thio-OMP, and 2-thio-OMP complex trajectories. For both the substrate and 4-thio-OMP complexes, the average distance between the two atoms is 4.6 Å, with 47% of the 150 configurations having values less than this average distance. For the 2-thio-OMP complex, this percentage is only 0.2%, with an average distance of 5.1 Å. In the 150−300 ps interval of the 2-thio-OMP complex trajectory, the percentage is comparable with a value of 2.7%. Overall, these results suggest that the loss of catalytic activity for the 2-thio-OMP ligand is due to a greatly reduced occupancy

Table 2. Statistical Data on Distances (in Å) between Nζ Lys72 and C5 of the Ligand As Sampled by Various ODCase−Ligand Complex Trajectories[a]

ligand	min	max	avg (SD)	% less than 4.6 Å
OMP	3.4	5.2	4.6 (0.3)	47.3
4-thio-OMP	3.7	5.4	4.6 (0.3)	46.7
2-thio-OMP	4.6	5.7	5.1 (0.2)	0.7

[a] Structures were sampled every picosecond in the 150−300 ps interval for OMP and 4-thio-OMP, and in the 850−1000 ps interval for 2-thio-OMP.

Table 3. Average Energetic Contributions to Enzyme Complex Formations with the 6-aza-UMP Inhibitor[a] (in kcal/mol) with Standard Errors of the Mean in Parentheses

	with charged Asp70		with neutral Asp70	
	$\epsilon_{int} = 1$	$\epsilon_{int} = 4$	$\epsilon_{int} = 1$	$\epsilon_{int} = 4$
$\langle\Delta E_{elec}\rangle$	107.5 (4.3)	26.9 (1.1)	22.0 (2.3)	5.5 (0.6)
$\langle\Delta E_{vdW}\rangle$	−31.0 (0.9)	−31.0 (0.9)	−32.9 (1.0)	−32.9 (1.0)
ΔG_{PB}	−54.2 (4.4)	−17.3 (1.0)	38.8 (2.0)	3.4 (0.5)
ΔG_{SA}	−4.2 (0.1)	−4.2 (0.1)	-4.2 (0.1)	-4.2 (0.1)
$-T\Delta S$[b]	20	20	20	20
ΔG_{bind}	38.2 (3.1)	−5.5 (0.8)	43.6 (2.1)	−8.2 (0.9)
ΔG_{bind}(exp)	−9.0			

[a] Fifteen configurations sampled every 10 ps from 150 to 300 ps in trajectory. [b] Estimated value based on published results for similarly sized ligands.[43]

of configurations that allow for efficient delivery of a proton by Lys72 to C5 relative to the cases of the substrate and 4-thio-OMP ligand.

Interestingly, similar results were obtained for C6-protonation. The average distance between Nζ of Lys72 and C6 of the ligand was 4.3 Å for the substrate complex trajectory, with 48.7% of the substrate complex configurations, 33.3% of the 4-thio-OMP complex configurations, and only 4% of the 2-thio-OMP configurations (5.3% for the 150−300 ps interval) with values less than this distance.

3.3. MM-PBSA. The combined molecular dynamics and continuum solvent model approach (MM-PBSA) of Srinivasan *et al.*[21] was performed to obtain the binding free energies for each enzyme−ligand complex in this study. Given the fact that use of a larger interior dielectric ($\epsilon_{int} = 4$) leads to a more realistic absolute ΔG_{bind} for highly charged species,[43] the electrostatic contributions to the binding free energy were computed using $\epsilon_{int} = 4$ as well as $\epsilon_{int} = 1$. Solute entropic contributions ($-T\Delta S$) to the binding free energy were assumed to be similar for all enzyme−ligand complexes and hence were not computed. An assumed entropic contribution of +20 kcal/mol was used, based on published results for similarly sized ligands.[45]

Computed binding free energies for the enzyme−(6-aza-UMP) complex, with both the neutral and anionic forms of Asp70, are shown in Table 3. Even though the absolute calculated free energies of binding are unrealistically positive for $\epsilon_{int} = 1$, they are reasonably close to experiment with $\epsilon_{int} = 4$, given the ∼20 kcal/mol expected contribution from the $-T\Delta S$ term for ligand binding.[45] Furthermore, both the OMP substrate and the unimolecular decarboxylation transition-state model (Figure 4) are computed to have significantly more favorable binding free energies than the 6-aza-UMP inhibitor, independent of the assumed dielectric model or protonation state. This argues against "ground-state destabilization" [13] since, if anything, the substrate is found to interact more favorably with the enzyme than the inhibitor, which lacks the negatively charged carboxylate group.

(45) Chong, L.; Duan, Y.; Wang, L.; Massova, I.; Kollman, P. *Proc. Natl. Acad. Sci. U.S.A.* **1999**, *96*, 14330−14335.

Table 4. Average Energetic Contributions to GS and TS Complex Formations with Neutral Asp70[a] (in kcal/mol) with Standard Errors of the Mean in Parentheses

	GS complex		TS complex	
	$\epsilon_{int} = 1$	$\epsilon_{int} = 4$	$\epsilon_{int} = 1$	$\epsilon_{int} = 4$
$\langle\Delta E_{elec}\rangle$	47.6 (4.6)	11.9 (1.2)	57.9 (4.7)	14.5 (1.2)
$\langle\Delta E_{vdW}\rangle$	−29.7 (1.5)	−29.7 (1.5)	−33.4 (1.3)	−33.4 (1.3)
ΔG_{PB}	−21.8 (4.6)	−14.7 (1.0)	−34.2 (4.7)	−18.1 (1.0)
ΔG_{SA}	−4.5 (0.1)	−4.5 (0.1)	−4.6 (0.0)	−4.6 (0.0)
$-T\Delta S$[b]	20	20	20	20
ΔG_{bind}	11.7 (2.5)	−16.9 (1.5)	5.6 (3.2)	−21.7 (1.0)
ΔG_{bind}(exp)	−8.3			

[a] Fifteen configurations sampled every 10 ps from 150 to 300 ps in trajectory. [b] Estimated value based on published results for similarly sized ligands.[43]

Table 5. Average Energetic Contributions to Enzyme Complex Formations with 2-thio-OMP[a] and 4-thio-OMP with Neutral Asp70[b] (in kcal/mol) with Standard Errors of the Mean in Parentheses

	2-thio-OMP complex		4-thio-OMP complex	
	$\epsilon_{int} = 1$	$\epsilon_{int} = 4$	$\epsilon_{int} = 1$	$\epsilon_{int} = 4$
$\langle\Delta E_{elec}\rangle$	59.9 (5.6)	15.0 (1.4)	45.0 (4.2)	11.3 (1.0)
$\langle\Delta E_{vdW}\rangle$	−26.8 (1.5)	−26.8 (1.5)	−29.4 (1.1)	−29.4 (1.1)
ΔG_{PB}	−51.7 (4.2)	−20.4 (0.9)	−32.9 (3.8)	−17.9 (0.9)
ΔG_{SA}	−4.5 (0.1)	−4.5 (0.1)	−4.7 (0.0)	−4.7 (0.0)
$-T\Delta S$[c]	20	20	20	20
ΔG_{bind}	−3.0 (2.6)	−16.7 (1.1)	−1.9 (2.6)	−20.7 (1.1)
ΔG_{bind}(exp)	−6.5		−6.7	

[a] Fifteen configurations sampled every 10 ps from 850 to 1000 ps in trajectory. [b] Fifteen configurations sampled every 10 ps from 150 to 300 ps in trajectory. [c] Estimated value based on published results for similarly sized ligands.[43]

Binding free energy contributions for the substrate and transition state to unimolecular decarboxylation are shown in Table 4 for the neutral form of Asp70 in the enzyme. The binding free energies of both the substrate and transition-state complexes are more favorable for the neutral form of Asp70 than the anionic form, regardless of the choice of interior dielectric constant (data not shown). Considering the results with the neutral Asp70, the binding free energy of the transition-state complex is 5−6 kcal/mol more favorable than that of the substrate complex with the neutral Asp70, comparable to the 2 kcal/mol stabilization noted by Wu *et al.*[16] This lack of differential stabilization of the ground state and transition state is inconsistent with ground-state destabilization, which would require a 20 kcal/mol difference between the destabilization of the ground state (18 kcal/mol) and stabilization of the transition state (−2 kcal/mol).[16]

Binding free energies for the 2-thio and 4-thio substrate analogues in complex with the neutral form of Asp70 of the enzyme are shown in Table 5. Although the calculated ΔG's are unusually favorable for the choice of dielectric constant $\epsilon_{int} = 1$, they are comparable to that of the unsubstituted substrate for $\epsilon_{int} = 4$, which is consistent with experimental data.[8] It is clear that there are difficulties in quantitatively applying MM-PBSA to highly charged ligands, but, nonetheless, our results provide evidence against ground-state destabilization of the substrate.

To this point, we have assumed Asp70 to be in its neutral state. Given the proximity of Asp70 (with an intrinsic pK_a of 4.0) to the orotate carboxylate group (intrinsic pK_a of 2.5), one would expect it to pick up a proton. Yet, several charged residues are also present in the active site (Lys72, Lys42, and Asp75B), which could have the effect of compensating for the strong repulsion expected between an anionic Asp70 and the orotate carboxylate group. To address this issue, we have

employed a new methodology that uses the MM-GBSA approach to calculate the pK_a's of ionizable groups (B. Kuhn, unpublished results). This method has led to an average error of 1.5 pK_a units for known pK_a's in hen egg white lysozyme when the computations were performed on a single trajectory (B. Kuhn, unpublished results). Due to the significant differences in local environment for the anionic and neutral states of Asp70, its pK_a was determined by taking the average of the results obtained using the trajectory with the anionic form of Asp70 and that with the neutral form of Asp70. The resulting pK_a of Asp70 is 7.7 ± 2.2, which is raised from its intrinsic value by $\sim$3−4 pK_a units.

4. Discussion and Conclusions

QM calculations performed here and by others[4,13] as well as experiments[1] find the activation barrier for the nonenzymatic decarboxylation of the OMP substrate to be in the range of 35−40 kcal/mol. For a simple unimolecular reaction where the C6−CO_2^- dissociates to leave an anionic base, it is hard to imagine what kind of noncovalent interactions could differentially stabilize the more charge-delocalized transition state relative to the reactant. Thus, several research groups[9,10,12,16] have invoked the concept of ground-state destabilization to explain the catalysis of decarboxylation by ODCase.

A ground-state destabilization of 18 kcal/mol has been reported by Wu *et al.*[16] on the basis of QM/MM calculations with a model where a severe repulsion exists between the anionic form of Asp70 and the substrate carboxylate. Using potential of mean force (PMF) free energy calculations, they determined the $\Delta G^{\ddagger}$ for the enzyme-catalyzed reaction to be 15 kcal/mol, in excellent agreement with that found experimentally. It should be be noted that Wu *et al.* used a system containing only *N*-methyl orotate in their QM solution calculations and a QM/MM system with C1′ linked by a classical link atom in their enzyme calculation. Since the solution PMF was not computed with the same QM/MM protocol, it is uncertain whether the inaccurate forces introduced by the link atom resulted in artifacts appearing in the PMF. In addition, Warshel *et al.*[17] have criticized the decision not to include Lys72 in the QM region of the QM/MM system due to its role in donating a proton in the concerted ground-state destabilization mechanism.

Our MD simulations of the enzyme−substrate complex show that Lys72 is well-positioned to deliver a proton to C5 or C6. However, C5-protonation has a lower activation barrier than C6-protonation, as determined by QM reaction energy profiles and QM-FE calculations. Furthermore, MM-PBSA binding free energy calculations of the enzyme−substrate, enzyme−transition state, and enzyme−inhibitor complexes show that there is little or no ground-state destabilization by the enzyme. Instead, Asp70 is preferentially protonated, as indicated by a computed pK_a of 7.7 ± 2.2. In principle, our pK_a calculations should be reasonably accurate, given the average error observed on similar systems. The large error of 2.2 pK_a units in our pK_a calculation for Asp70 is most likely due to the significant difference between the complex structure with the neutral Asp70 and that with the anionic Asp70, as observed in the MD simulations. Furthermore, the MD simulation of the enzyme−substrate complex remains closer to the crystal structure of the inhibitor-bound enzyme with the neutral state of Asp70. This observation, combined with our pK_a calculation and the fact that the binding affinity of the enzyme−substrate complex is more favorable with a neutral Asp70 than with an anionic Asp70, supports the assertion that Asp70 is neutral. The preference of Asp70 to be in a neutral state has precedent in enzyme systems such as HIV protease, where it is likely that the catalytically active form has one neutral and one charged aspartic acid residue.[46−48] Based on the role of Asp70 in stabilizing the substrate carboxylate group in the correct geometry, its role in controlling the position of Lys72 with the help of Asp75B from the adjacent monomer, and its total conservation in all known forms of ODCase, we would expect Asp70 to be important for catalysis. We would also expect that a D70N mutant would retain some catalytic activity. In solution, the mechanism of decarboxylation is different, since any excess protons would first protonate the substrate carboxylate group, blocking decarboxylation through the C5-protonation mechanism. The enzyme has thus created a microenvironment that protects the substrate carboxylate group from protonation through hydrogen bonding with Asp70, enabling facile decarboxylation through protonation of C5.

To relate our calculations to the observed $\Delta G^{\ddagger}$ of 15 kcal/mol,[1] the QM-FE calculations for C5-protonation would have to lead to a significant lowering of the barrier to protonation and stabilization of the C5-protonated intermediate over those found in the gas phase. Our calculations do show this, although the quantitative stabilization is clearly too large. Postulating a more plausible barrier to protonation of $\sim$10 kcal/mol that accounts for the observed stabilization of the enzyme environment and proton tunneling effects, we can construct a free energy profile for the reaction that explains the experimental data. As shown in Figure 10, the barrier to decarboxylation of the C5-protonated species (Figure 9) would lead to an effective barrier of $\sim$15 kcal/mol for decarboxylation. We emphasize that we have not precisely calculated the free energy profile in Figure 10. Thus, all that we can claim at this point is the plausibility of this mechanism.

Our proposed mechanism has similarities to the mechanism proposed by Beak and Siegel,[2] in which protonation of the substrate at O2 was the critical step to catalysis, and to that proposed by Lee and Houk,[4] in which O4-protonation was instrumental. In our view, supported by the greater intrinsic proton affinity of C5 than O2, O4, or C6 of orotate, the smaller energy barrier of C5-protonation than C6-protonation, the modest calculated barrier for methylammonium ion (as a model of Lys72) to orotate proton transfer, and the subsequent smaller barrier for decarboxylation once C5 is protonated, the mechanism here is more consistent with the evidence from Ehrlich *et al.*[5] that suggests equilibrium pre-protonation followed by a rate-limiting decarboxylation.

Recent ^{15}N kinetic isotope effect experiments[49] have implied that no bond order changes take place at N1, thereby ruling out mechanisms such as the one proposed by Beak and Siegel[2] which involve formation of an ylide intermediate. To assess the magnitude of bond order change at N1, we computed the N1 ^{15}N equilibrium isotope effect on C5-protonation using both orotate and *N*-methyl orotate. The computed ^{15}N equilibrium isotope effects for orotate and *N*-methyl orotate are 0.994 and 0.995, respectively. Experimentally, the intrinsic ^{15}N isotope effect for the enzyme-catalyzed reaction was determined to be 1.007, while the observed isotope effects for model compounds *N*-methyl picolinic acid and picolinic acid were found to be 1.007 and 0.995, respectively (extrapolated to 298 K).[49] The

(46) Wang, Y.; Freedberg, D.; Yamakazi, T.; Wingfield, P.; Stahl, S.; Kaufman, J.; Kiso, Y.; Torchia, D. *Biochemistry* **1996**, *35*, 9945−9950.
(47) Luo, R.; Head, M.; Moult, J.; Gilson, M. *J. Am. Chem. Soc.* **1998**, *120*, 6138−6146.
(48) Trylska, J.; Antosiewicz, J.; Geller, M.; Hodge, C.; Klabe, R.; Head, M.; Gilson, M. *Protein Sci.* **1999**, *8*, 180−195.
(49) Rishavy, M.; Cleland, W. *Biochemistry* **2000**, *39*, 4569−4574.

normal isotope effect for *N*-methyl picolinic acid is interpreted as arising solely from the loss of N−C−C and N−C−C−O vibrational modes in the decarboxylation step, while the inverse effect for picolinic acid is interpreted as being due to the product of a similar normal value for the decarboxylation step and a larger inverse equilibrium value arising from the protonation of N1 to give the quaternary ammonium ion prior to the decarboxylation step. The overall ^{15}N isotope effect in our mechanism will be the product of our calculated value of 0.995 for the equilibrium protonation at C5 and a normal secondary kinetic isotope effect for the subsequent decarboxylation step due to the loss of the same vibrational modes as in the two model compounds. Although the identity of the ^{15}N isotope effects in the enzyme and *N*-methyl picolinic acid was used as an argument against the pre-equilibrium formation of the ylide intermediate with a much larger predicted inverse isotope effect of 0.97, the value of 1.007 observed in the enzyme would also be consistent with our much smaller inverse isotope effect (0.995) multiplied by a slightly larger normal effect for the decarboxylation step than the value observed for the *N*-methyl picolinic acid model. The fact that the ^{13}C isotope effect for the enzymatic reaction (1.049) is substantially larger than that observed for the model reaction (1.028) supports the idea that the ^{15}N effect for the decarboxylation step in the enzyme is larger than that for the model. Consistent with these results are the observed opposite changes in the N1−C6 and N1−C2 bond lengths upon C5-protonation (1.37 Å → 1.28 Å and 1.35 Å → 1.42 Å, respectively) as well as the fact that there is little or no stabilization of C5-protonation by resonance delocalization effects due to N1, as indicated by an increase in PA upon replacing N1−H of orotate by CH_2.

The possibility of a significant involvement of C5 in the mechanism has been explored by a number of kinetic isotope effect experiments. Even though the results of these experiments are not suggestive by themselves of an important role for C5 in the mechanism, our proposed mechanism is consistent with the experimental data.

Acheson *et al.*[6] found no 5-D isotope effect on either k_{cat} (0.99 ± 0.06) or k_{cat}/K_M (1.00 ± 0.06). Since the hybridization does not change at C5 during the loss of CO_2, no secondary isotope effect is expected for the decarboxylation step. However, due to the $sp^2 \rightarrow sp^3$ change upon protonation at C5 in the first step of our mechanism, one would expect an inverse secondary isotope effect that would be observed as an overall isotope effect on k_{cat} and k_{cat}/K_M. We thus computed the isotope effect expected upon 5-D substitution from the vibrational frequencies of the isotopically labeled and unlabeled versions of orotate and of the corresponding C5-protonated intermediate. This approach (see Methods) has reproduced measured isotope effects in many studies on enzyme mechanisms, with the most recent by Fitzpatrick,[50] Houk,[51] and Schramm.[52] Our calculations found a deuterium equilibrium isotope effect (k_H/k_D) of 1.012 ($\phi_{orotate} = 0.950$ and $\phi_{intermediate} = 0.938$ relative to water). This value is within experimental error of the values found by Acheson *et al.*[6] The absence of a significant isotope effect may be due to the electrostatic attraction between the hydrogen on the C5 and the carboxylate group, which could constrain the C5−H bond in such a way that the vibrational frequency of its out-of-plane bending motion is much higher than usual, thereby compensating for any inverse isotope effect.

Shostak and Jones found that F-substitution at C5 increased k_{cat} by 30-fold but reduced K_M by roughly the same amount, leading to an overall k_{cat}/K_M comparable to that for unsubstituted OMP.[8] To examine the consistency of our mechanism with this result, we carried out calculations to assess the effect of 5-F substitution on both the C5-protonation and decarboxylation steps in our proposed mechanism. As shown in Figure 8, the C5 PA decreases by 6 kcal/mol. On the other hand, the barrier to decarboxylation was computed to be only 4 kcal/mol, in contrast to the 10 kcal/mol found with the unsubstituted OMP substrate. These two results—reduction of the proton affinity and increase in the facility of decarboxylation—make qualitative sense, given the electron-withdrawing nature of the fluorine. While these calculations do not consider the environment of the enzyme, they suggest that, through raising the energy of the intermediate but diminishing the barrier to decarboxylation, the overall effective barrier (see Figure 10) remains approximately the same, leading to an observed k_{cat}/K_M that is similar to that of the unsubstituted OMP. In addition, an MD simulation of the enzyme in complex with the 5-F substrate analogue has revealed that the distance between Nζ of Lys72 and C5 of the ligand throughout the 150−300 ps interval averages only 3.6 Å, which is shorter than the average distance between the two atoms in the enzyme−OMP complex trajectory and could rationalize the greater k_{cat} for the 5-F analogue.

Shostak and Jones also found that the 5-aza substrate analogue was a good substrate for ODCase, but that the 5-Cl and 5-Br analogues were inhibitors.[8] Our calculations for the unsubstituted substrate and the 5-F analogue suggest that the 5-Cl and 5-Br analogues would also have PAs comparable to that of the unsubstituted substrate, as well as a low barrier to decarboxylation, as found for the unsubstituted substrate. Thus, it is hard to explain why the 5-Cl and 5-Br analogues are not substrates, but perhaps their larger size and greater hydrophobicity cause them to move toward the hydrophobic region of the binding site (away from the four charged residues, thus placing the C5 farther from the Nζ of Lys72). Clearly, further calculations or experiments (e.g., solving the crystal structure of the enzyme in complex with either its 5-Cl or 5-Br inhibitor) are necessary to sort this out.

Finally, our mechanism is consistent with the fact that replacement of O2 with sulfur has a large effect on k_{cat}, reducing it by more than 4−5 orders of magnitude, whereas replacement of O4 has little effect on k_{cat}.[8] We have shown that the energies for C5-protonation and subsequent decarboxylation are little affected by O4 → S4 or O2 → S2 substitution, but the structure of the S2-substituted complex is significantly different from that of the substrate or the S4-substituted complex. Indeed, MD simulations of 2-thio-OMP show that its phosphoribosyl group occupies a significantly different position in the active site than the OMP substrate or 4-thio-OMP, leading to a much less favorable orientation of the orotate ring for protonation of C5 by Lys72. This observation ties in nicely with the results of Wolfenden *et al.*,[53] which show a greater than 10^7-fold reduction in the k_{cat}/K_M upon removal of phosphoryl contacts with Tyr206 and Arg203 in the yeast enzyme via mutations to alanine residues. In our proposed mechanism, the O2 → S2 substitution places the substrate in a position where it is much less favorable for the lysine residue to protonate C5, thus significantly increasing the barrier to enzyme catalysis.

(50) Moran, G.; Derecskei-Kovacs, A.; Hillas, P.; Fitzpatrick, P. *J. Am. Chem. Soc.* **2000**, *122*, 4535−4541.
(51) Tantillo, D.; Houk, K. *J. Org. Chem.* **1999**, *64*, 3066−3076.
(52) Chen, X.; Berti, P.; Schramm, V. *J. Am. Chem. Soc.* **2000**, *122*, 6527−6534.
(53) Miller, B.; Snider, M.; Short, S.; Wolfenden, R. *Biochemistry* **2000**, *39*, 8113−8118.
(54) Ferrin, T.; Huang, C.; Jarvis, L.; Langridge, R. *J. Mol. Graphics* **1988**, *6*, 13−27.

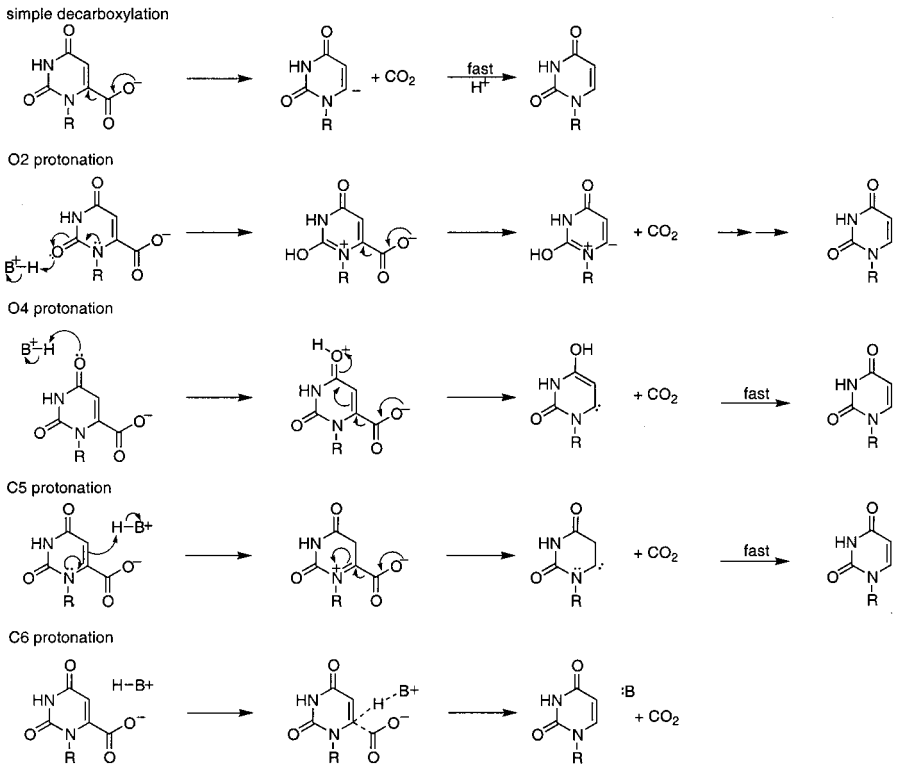

Figure 12. Reaction mechanisms considered in this study.

Our mechanism makes a rather interesting prediction for the enzyme-catalyzed reaction: if it is carried out in D_2O, the product could have some amount of deuterium at C5 as well as complete deuteration at C6. Simple unimolecular cleavage suggested by Wu *et al.*, O4-protonation suggested by Lee and Houk, and C6-protonation mechanisms suggested by Appleby *et al.* and Harris *et al.* would not incorporate any D at C5. Thus, product analysis by NMR or mass spectroscopy could shed light on our proposed mechanism. On the other hand, if the proton delivered by the lysine residue is the one that is preferentially removed or transferred from C5, once the CO_2 departs from the substrate, one could see significantly less than 50% D at C5 after the reaction. There are many precedents for such regioselectivity in enzyme reactions, such as in triose phosphate isomerase, where Glu165 always abstracts the pro-R hydrogen at C1 and delivers the proton to the *re* face of C3. In ODCase, one face of the bound ring has the hydrophilic groups such as Lys72 and Asp70 and the other, mainly hydrophobic side chains (e.g., so the H(D) lost from C5 could predominantly be the D).

To summarize, an observation of D-incorporation at C5 upon running the enzymatic reaction in D_2O would strongly support our mechanism, but the absence of significant D at C5 would not rule it out. Once the CO_2 of the substrate leaves, there are two hydrogens at C5 and none at C6. To probe whether the substrate reaches its more stable state with one hydrogen at C5 and one at C6 by an intramolecular C5 → C6 hydride transfer, we calculated the energies for this process at the MP2/6-31+G*//HF/6-31+G* level and found the barrier for it to be 28 kcal/mol. Thus, it is very likely that the hydrogen on C5 transfers to Lys72, particularly given that the loss of CO_2 dramatically reduces the favorable energy for C5-protonation (Figure 8). Independently, the neutral Asp70 or a water molecule donates a proton to C6, given the instability of the carbanion at C6, thereby regenerating the system for another round of catalysis. Thus, once the C6−CO_2 bond breaks, both deprotonation of C5 and protonation of C6 by the environment would occur in an independent and rapid manner.

We have considered five reaction mechanisms for the decarboxylation of OMP catalyzed by ODCase (Figure 12). The first is simple decarboxylation, in which ground-state destabilization drives catalysis. Although supported by the QM/MM and free energy calculations by Wu *et al.*,[16] it is nonintuitive for such a mechanism to produce such a large catalytic effect, since the ground state and transition state are similarly charged. Indeed, the free energy calculations by Wu *et al.* found that discharging the ground state and transition state gave similar $\Delta\Delta G^{\ddagger}$'s, although their calculated reaction profile reproduces a very large effect of the enzyme. Likewise, our MM-PBSA free energy calculations found similar binding free energies for the enzyme-bound ground state and transition state. These two pieces of data argue against preferential stabilization of the transition state or destabilization of the ground state for decarboxylation. Furthermore, our pK_a calculations have found that Asp70 prefers to be neutral in the presence of the substrate rather than creating electrostatic stress with the substrate in its anionic form.

The other four mechanisms for ODCase suggest that the enzyme mechanism is fundamentally different than in solution, with protonation of either O2, O4, C6, or C5 preceding decarboxylation. Given the location of Lys72 in the enzyme, the environment of O2 and O4, and the fact that O4 → S4 has little effect on k_{cat}, the O2-protonation and O4-protonation mechanisms are unlikely. During our MD simulations, Lys72 tended to be approximately equidistant from C5 and C6, suggesting that this group was reasonably located to protonate either site.

Our QM calculations found that C5-protonation is favored over C6-protonation, although our QM energy profiles do not consider any proton tunneling effects that would presumably lower the barriers to protonation. C6-protonation would immediately lead to decarboxylation, whereas C5-protonation

would lead to a metastable intermediate, whose barrier to loss of CO_2 is only ~10 kcal/mol (Figure 9). Thus, our calculations do not fully rule out C6-protonation since we have not performed FE calculations on an intermediate with C6-protonation. It is conceivable that environmental effects would also stabilize protonation at this position. Based on our lower calculated barrier for C5-protonation and the implication by Ehrlich *et al.*[5] of an equilibrium protonation step, our results would favor C5- over C6-protonation.

We should note, however, that accurate calculations on the enzyme environment effect were not performed along the entire reaction profile. Furthermore, Warshel *et al.*[17] obtained very large TS stabilization in a consistent calculation that involved both energy profile and binding calculations. This might be significant since the intermediate in the calculations by Warshel *et al.* (uridine$^-$ + Lys72$^+$ + CO_2 + Asp70$^-$) is similar to ours (uridine$^-$ + Lys72$^+$ + CO_2 + Asp70).

In conclusion, we have presented results using a wide variety of computational methods—QM calculations, classical free energy calculations, molecular dynamics simulations, and MM-PBSA free energy calculations—to support the hypothesis that ODCase has a different mechanism of decarboxylation than that found in the reference reaction in solution. In the enzyme mechanism, we propose that C5-protonation precedes decarboxylation. There are a number of uncertainties in our results, most of which arise from not having the exact geometry of the enzyme−substrate complex and the large size of this enzyme system, which precludes the use of accurate long-range (e.g., particle mesh Ewald) electrostatics. Thus, the mechanism of ODCase is far from resolved. Nonetheless, some of the structure/activity relationships (high rate of catalysis of the 4-thio substrate analogue, but low activity of the 2-thio analogue; and the high rate of catalysis of the 5F analogue, but not the 5Cl analogue) argue for a mechanism which involves precise placement of groups in the enzyme (e.g., proton transfer) rather than just generalized electrostatic stabilization/destabilization during unimolecular decomposition.

Acknowledgment. T.-S.L. and L.T.C. contributed equally to this work. This article is dedicated to Peter A. Kollman, a wonderful mentor and friend who succumbed to cancer during the lengthy review process, but whose enthusiasm to see this work published never waned. The authors thank B. Kuhn for his assistance and methodology for computing pK_a values, and M. Saunders for providing the QUIVER program. We also thank S. Miller and I. Kuntz for helpful discussions. This work was supported in part by a National Institutes of Health (NIH) Grant (GM29072) to P.A.K., an NIH training grant to T.-S.L. (F32-GM19410-02), a National Science Foundation (NSF) Fellowship to L.T.C., and an NIH training grant (GM08284) to J.D.C. J.D.C. is a Howard Hughes Medical Institute Predoctoral Fellow. Graphics were provided by the Computer Graphics Laboratory, University of California, San Francisco (T. Ferrin, P.I., NIH P41 Grant RR-01081). NSF is acknowledged for providing computational resources at the National Center for Supercomputing Applications, University of Illinois at Urbana−Champaign.

Supporting Information Available: Ligand force field parameters not present in the Cornell *et al.* force field[33] (PDF). This material is available free of charge via the Internet at http://pubs.acs.org.

JA011096F